

ASSESSING EROSION CONTROL SUITABILITY WITH NORMALIZED DIFFERENCE
INFRARED INDEX IN A SEMI-ARID WATERSHED

By

NELLY RUBIO

MASTER OF SCIENCE
GEOGRAPHIC INFORMATION SYSTEMS TECHNOLOGY
FINAL PROJECT

THE UNIVERSITY OF ARIZONA

2025

ACKNOWLEDGMENTS

I extend heartfelt thanks to my partner for their insightful feedback and unwavering encouragement, which inspired me to embark on this journey. I also deeply appreciate the faculty of the GIST program for fostering a rich educational experience and promoting a thoughtful understanding of work-life balance.

TABLE OF CONTENTS

	<u>page</u>
ACKNOWLEDGMENTS.....	2
LIST OF TABLES.....	5
LIST OF FIGURES.....	6
LIST OF ABBREVIATIONS.....	8
ABSTRACT.....	9
INTRODUCTION.....	10
Historical Impacts and the Loss of Hydrologic Function	10
One Rock Dams	11
Hydrologic and Biogeochemical Importance of Ephemeral Streams	12
Vegetation Response and Drought Resilience via RDS	12
Remote Sensing Applications.....	13
Quantitative vs Qualitative	15
Objective.....	15
METHODS	17
Study Area	17
Data	19
Data Processing	21
Summary.....	21
Precipitation Analysis	22
Landsat Imagery Collection	23
R Script Analysis.....	24
NDII Analysis.....	24
Digital Elevation Model Preparation	25
ArcGIS Model Builder	25
Watershed Delineation	27
Cost Surface Development.....	28
Slope and Velocity Suitability Criteria.....	29
NDII Reclassification for Infiltration Zones.....	31
Final Suitability Raster and Prioritization Zones	31
Validation Methods.....	32
Priority Zone Extraction	33
NDII Value Extraction	33
Rain Gauge Association.....	33
Integrated Comparison.....	34

RESULTS.....	35
Composite Suitability for ORD Placement in WGEW.....	35
Seasonal NDII Variation and Infiltration Patterns	35
Logistical Accessibility: Ruggedness and Road Proximity Analysis	38
Geomorphic Parameters for ORD Suitability	39
Composite Suitability Zones for ORD Installation.....	41
NDII-Based Moisture Validation Using Rain Gauge Data.....	43
CONCLUSION	45
Summary	45
Study Objectives & Outcomes	45
(1) Can NDII be used to identify zones with low soil moisture and high suitability for ORD placement?.....	45
(2) Do NDII trends at identified zones correlate with precipitation data collected from rain gauges?	45
Future Enhancements.....	46
Implications & Field Validation	46
LIST OF REFERENCES	48
APPENDIX A.....	51
METADATA TABLES.....	51

LIST OF TABLES

<u>Table</u>	<u>page</u>
Table 1. Data table summarizing joined attributes for NDII-prioritized points. Each row represents a priority location linked to its nearest rain gauge, including NDII change values for 2020 and 2022, rain gauge ID, spatial distance to the gauge (in meters), and aggregate annual precipitation totals (in centimeters). ..	44
Table A1. Shuttle Radar Topography Mission (SRTM) 1 Arc-Second Global DEM	51
Table A2. Landsat 8–9 OLI/TIRS Collection 2 Level-2 Surface Reflectance Imagery ...	51
Table A3. SWRC Flume and Rain Gauge Locations.....	51
Table A4. Arizona Rivers Layer.....	52
Table A5. Primary and Secondary Roads (TIGER/Line 2024)	52
Table A6. Rain Gauge Data – Tucson ARS Digital Aggregate Portal	53

LIST OF FIGURES

<u>Figure</u>	<u>page</u>
Figure 1. Study area includes the Walnut Gulch Experimental Watershed, situated near Tombstone, Arizona, USA—bounded to the west by the San Pedro River and to the east by the Dragoon Mountains.....	18
Figure 2. Methodology summary of analysis for ORD placement suitability.....	22
Figure 3. Total annual precipitation (in centimeters) derived by averaging aggregate rain gauge measurements across all stations for each calendar year. These values were used to identify the driest and wettest years included in the NDII analysis.	23
Figure 4. Workflow constructed in ArcGIS Pro ModelBuilder illustrating the automated sequence for hydrological and suitability analysis within the WGEW.	26
Figure 5. Hydrologically derived polygon showing the final watershed boundary delineation for WGEW.	28
Figure 6. Validation model illustrating the spatial and statistical workflow used to assess the effectiveness of NDII as a proxy for identifying low-infiltration zones within the WGEW.....	32
Figure 7. Spatial visualization of 1000-meter buffer zones surrounding NDII-prioritized erosion control points used to identify nearby rain gauges for precipitation comparison and validation.....	34
Figure 8. Annual rasters depicting NDII-based classification changes derived from seasonal comparisons between pre- and post-monsoon periods.....	36
Figure 9. Distribution of NDII Classification Categories Within the WGEW from 2020 to 2022. The predominance of stable classifications reflects persistently dry conditions across much of the watershed and underscores the limited hydrologic response typical of semi-arid environments.	37
Figure 10. Low infiltration zones identified through NDII analysis, based on combined 2020 and 2022 rasters where values consistently remained within or below stability thresholds.....	38
Figure 11. Cost surface raster depicting suitable areas (green) with favorable accessibility based on terrain ruggedness and proximity to road networks.	39
Figure 12. Ideal slope raster identifying zones with gradients between 2% and 4% across the WGEW, suitable for one rock dam placement.	40

Figure 13. Stream velocity raster highlighting ideal segments within the WGEW where flow rates range between 0.2 m/s and 2.0 m/s, suitable for erosion control structure placement. 41

Figure 14. Composite suitability raster identifying high-priority points for ORD placement within WGEW, derived from slope, stream velocity, soil moisture, and accessibility metrics. 42

Figure 15. Terrain-based priority zone raster for ORD placement within the WGEW excluding low infiltration zones and focusing solely on slope, ruggedness, and accessibility criteria. 43

LIST OF ABBREVIATIONS

CLIMATE	Climatic Generator (often used to refer to climate simulation modules or tools in EPIC and WEPP workflows)
CREAMS	Chemicals, Runoff, and Erosion from Agricultural Management Systems
DEM	Digital Elevation Model
ECS	Erosion control structures
EPIC	Environmental Policy Integrated Climate
KINEROS	Kinematic Runoff and Erosion Model
LTAR	Long-Term Agroecosystem Research
NDII	Normalized difference infrared index
NDVI	Normalized difference vegetation index
NIR	Near infrared
ORD	One rock dams
RDS	Rock detention structures
RUSLE	Revised Universal Soil Loss Equation
SPUR	Simulation of Production and Utilization of Rangelands
SRTM	Shuttle Radar Topography Mission
SWIR	Short wave infrared
SWRC	Southwest Watershed Research Center
USDA	United States Department of Agriculture
USGS	United States Geological Survey
WEPP	Water Erosion Prediction Project
WGEW	Walnut Gulch Experimental Watershed

ABSTRACT

Accurate assessment of soil moisture and infiltration capacity is essential for watershed management in semi-arid regions like Southern Arizona, USA. This study investigates the use of the Normalized Difference Infrared Index (NDII) to identify areas of low infiltration within the Walnut Gulch Experimental Watershed (WGEW), focusing on the driest (2020) and wettest (2022) monsoon seasons between 2015 and 2025. NDII, a remote sensing index sensitive to vegetation water content, serves as a proxy for root zone soil moisture. This study uses Landsat 8/9 imagery to analyze NDII changes between May and October and classify areas from low to high infiltration response. Comparing NDII change values across contrasting years highlights zones with persistent low infiltration. Identifying these areas is the first step toward developing a restoration strategy for semi-arid watersheds. A multi-criteria suitability analysis—incorporating slope, terrain ruggedness, road accessibility, and soil moisture data—prioritizes locations for erosion control structures (ECS). ECS offer a cost-effective restoration method by reducing water velocity and enhancing infiltration potential. Integrating NDII dynamics with hydrological and terrain factors provides a scalable, data-driven framework to support sustainable watershed restoration in arid environments.

Keywords: NDII, Soil Infiltration, Watershed Restoration, Erosion Control Structures, Landsat 8/9

INTRODUCTION

Watershed management in semi-arid regions is critical to sustaining water availability for both ecological systems and human use. In these environments, stream erosion and degradation diminish hydrologic functionality, leading to reduced soil infiltration and compromised water retention. Drawing from the traditional ecological knowledge of Indigenous communities, land managers have long employed rock detention structures (RDS) or erosion control structures (ECS) as cost-effective, nature-based solutions to rehabilitate degraded landscapes (Gooden & Pritzlaff, 2021). These interventions promote sediment deposition and enhance soil infiltration, ultimately restoring ecological resilience. Environmentalist Aldo Leopold, writing in *The Virgin Southwest* (1933), recognized the alarming rise of erosion in New Mexico and the broader Southwest, calling on the public to embrace ecological science as a means of preserving land health and continuity. Located on an alluvial fan in southeastern Arizona, the Walnut Gulch Experimental Watershed (WGEW) exemplifies many of these challenges, serving as a key study site for Watershed management (Southwest Watershed Research Center, 2003).

Historical Impacts and the Loss of Hydrologic Function

Before the introduction of cattle grazing, timber extraction, and beaver hunting, cienegas—wetland ecosystems—once flowed through the biodiverse deserts of the Southwest. According to Cuenca Los Ojos, Borderlands Restoration Network, and the Biophilia Foundation (2021), the region has since entered a “self-perpetuating cycle of degradation.” Colonization triggered widespread land-use changes that compromised the delicate balance sustaining these systems. The removal of keystone species and vegetation, combined with annual monsoon rains, accelerated channel erosion, carving

deep head cuts into the landscape. This not only lowered soil infiltration capacity but also disrupted the subsurface water table. As vegetation vanished, the soil hardened—dry and compacted—fueling rapid runoff and reinforcing a destructive feedback loop of ecological decline.

One Rock Dams

A variety of RDS or ECS can be implemented in watersheds depending on geomorphology and landform characteristics. Given that the WGEW is situated on an alluvial fan, the terrain primarily consists of unconsolidated alluvium deposits —ideal for promoting infiltration and sediment deposition. These deposits can experience large transfer flows during monsoon rainfall. In response to erosion challenges in semi-arid environments, Bill Zeedyk developed techniques that center on hand-built rock structures—now widely known as Zeedyk structures — to offer nature-based solutions rooted in traditional land stewardship. Among these, the one rock dam (ORD) is frequently used in upstream zones to slow surface runoff, capture sediment, enhance infiltration, and support vegetative establishment. As Maestas et al. (2018) explain, “an ORD is made of many rocks fit tightly together, but gets its name from being only one rock high (generally no more than a third the height of the bankfull channel)” (p. 20). These structures, framed by Norman et al. (2021) as green infrastructure, offer ecosystem services including water and habitat provisioning, nutrient cycling, erosion control, and flood mitigation. This project applies site-specific placement standards for ORDs to improve hydrologic resilience and ecological function across the WGEW. The strategic placement of ORDs in alluvial fan terrain aligns with both geomorphic suitability and long-standing land stewardship traditions practiced by Indigenous communities across the Southwest.

Hydrologic and Biogeochemical Importance of Ephemeral Streams

Watershed health supports diverse plant and animal communities, particularly in semi-arid regions where ephemeral and intermittent streams dominate the hydrologic network. These dynamic systems perform essential biogeochemical functions, including the storage and cycling of nitrogen, phosphorous, and organic carbon. Jacobson et al. (2000) observed that “organic carbon, nitrogen and phosphorous were correlated with silt content, and silt deposition patterns influenced patterns of moisture availability and plant rooting, creating and maintaining micro-habitats for various organisms.” (p.1). Such silt-mediated nutrient retention enhances soil fertility and vegetation resilience. Similarly, ephemeral streams in the American Southwest contribute to watershed function by facilitating nutrient cycling, sediment transport, and groundwater recharge, despite their intermittent flow regimes (Levick et al., 2008). However, the episodic nature of precipitation in arid landscapes leads to intense runoff events that mobilize these sediments, often degrading stream productivity and habitat stability. RDS can counteract this effect by capturing sediment during rainfall events, thereby promoting channel stabilization, and restoring biogeochemical function.

Vegetation Response and Drought Resilience via RDS

Due to the episodic nature of precipitation in the American Southwest, relying solely on rainfall for water availability introduces ecological instability. Enhancing soil moisture retention reduces evaporative losses and promotes increased vegetation coverage, thereby strengthening drought resilience. Using normalized difference vegetation index (NDVI), Gooden and Pritzlaff (2021) demonstrated elevated greenness in areas where RDS had been installed—even during periods of limited rainfall. These findings support a shift toward proactive solutions that improve infiltration and plant-soil

interactions, rather than remaining dependent on variable precipitation. As Gooden and Pritzlaff (2021) note, “Land managers also note that storing water in vegetated soil is preferable to storing water in open ponds because it is subject to less evaporation and therefore provides another adaptation to drought” (p. 7) reinforcing the value of nature-based strategies in arid environments. Similarly, Watts et al. (2007) describes the extreme dryness of southwestern landscapes prior to monsoon rains and highlights how post-rain increases in greenness drive evapotranspiration and moderate surface temperatures. These NDVI-driven fluxes demonstrate the ecological importance of vegetation in regulating energy exchanges and sustaining landscape resilience. Improving conditions for vegetation growth, particularly within watersheds like Walnut Gulch, is therefore vital for both hydrological stability and ecosystem health.

Remote Sensing Applications

Remote sensing plays a critical role in watershed management, with NDVI widely employed to monitor changes in vegetation response. However, this project utilizes the normalized difference infrared index (NDII) as a proxy for soil moisture — a crucial metric for assessing restoration success. While most landscape monitoring evaluates performance based on vegetative outcomes, NDVI is typically used to assess vegetation greenness, relying on Landsat red and near-infrared (NIR) bands. Since healthy vegetation absorbs red light and reflects NIR, the contrast between these bands serves as a reliable indicator of plant vigor. To quantify leaf water content, Hardisky et al. (1983) introduced NDII, which integrates NIR and shortwave infrared (SWIR) bands from Landsat imagery. Well-watered vegetation reflects more NIR and absorbs more SWIR, whereas dry vegetation exhibits the reverse pattern. As a result, NDII serves not

only as an indicator of canopy water content but also supports drought monitoring applications. According to Sriwongsitanon et al. (2016), “one would expect a direct relation between NDII and root zone moisture deficit. The deficit again is a direct function of the amount of moisture stored in the root zone” (p. 2). Given that soil moisture reflects infiltration efficiency, NDII offers a valuable, gauge-independent method for evaluating restoration outcomes—particularly in regions lacking dense hydrological instrumentation.

Although NDVI is commonly used to detect vegetation increase and inverted to highlight areas of low vegetation cover—often interpreted as indicators of reduced water availability. Identifying zones of persistent low soil moisture may be more informative for locating regions with low infiltration potential. In this context, NDII offers enhanced diagnostic capacity—not only for detecting low-moisture zones, but also for evaluating the success of ECS such as ORD installations. As noted by Wilson & Norman (2018), NDII is especially sensitive in cattle-grazed landscapes because it measures canopy moisture rather than overall greenness. This distinction is critical in the WGEW, a designated site within the Long-Term Agroecosystem Research (LTAR) Grazing Land network—a national program focused on sustainable agricultural production (Heilman et al., 2024). Grazing often reduces leaf area and alters spectral reflectance in ways that compromise NDVI’s reliability. In contrast, NDII remains effective under these conditions by detecting subtle changes in canopy moisture even where vegetation is sparse. These characteristics make NDII a valuable remote sensing tool for assessing soil moisture dynamics and restoration success in grazed arid lands.

Quantitative vs Qualitative

Quantitative assessments of watershed restoration via RDS remain scarce despite widespread qualitative endorsement. While anecdotal accounts highlight the effectiveness of RDS installations, land managers lack systematic methods to identify optimal placement zones and quantify ecological impact.

Common RDS types—including gabions, check dams, ORDs, and trincheras—are widely used in semi-arid landscapes but lack robust empirical validation. Norman (2020) emphasizes the urgent need for unbiased scientific data to educate land managers and inform policy. In related research, Wilson and Norman (2018) observed enhanced vegetative greenness surrounding gabion installations, with effects detectable up to 5 km downstream and 1 km upstream. Complementary findings by Polyakov et al. (2014) showed that loose rock check dams in the Santa Rita Experimental Range reduced runoff from small storms by 60% and retained approximately 75 tons of sediment over four years. Collectively, these studies identify vegetation response, runoff moderation, and sediment retention as key metrics for evaluating RDS performance—highlighting the importance of integrating hydrologic monitoring with remote sensing for comprehensive restoration analysis.

Objective

This study investigates the potential of NDII to prioritize locations for RDS or ECS—specifically ORDs—based on infiltration potential within the WGEW. It addresses two key research questions: (1) Can NDII be used to identify zones with low soil moisture and high suitability for ORD placement? (2) Do NDII trends at identified zones correlate with precipitation data collected from rain gauges?

To enhance replicability and scalability, this study integrates remote sensing—specifically NDII-based soil moisture analysis—to establish a framework for ORD placement in erosion-prone watersheds. Using Landsat imagery from 2020 to 2022, the study quantifies temporal changes in soil moisture and overlays geomorphic suitability and accessibility metrics—slope, ruggedness, and road access—to delineate priority zones for restoration intervention. By integrating remote sensing proxies with terrain-based modeling, this work contributes to the development of scalable, gauge-independent frameworks for watershed restoration in semi-arid environments. This approach aims to support land managers by offering an evidence-based framework for ORD deployment that is both transferable across landscapes and adaptable to varying levels of instrumentation.

METHODS

Study Area

This study was conducted within the WGEW, a semi-arid research watershed located in southwestern Arizona, USA (Figure 1). The watershed spans 150 square kilometers and surrounds the historic southwestern town of Tombstone. Geographically, WGEW lies within the Upper San Pedro River Basin and functions as an ephemeral tributary to the San Pedro River, which flows northward through Sonora, Mexico and Arizona. Entering the river from the east, Walnut Gulch contributes episodic runoff generated exclusively by summer convective thunderstorms. Geologically, WGEW is nestled in a basin-and-range physiographic province and is described by Osterkamp and Nichols (2006) as “an actively eroding alluvial-fan surface” (p. 5). The geologic material of the watershed is largely comprised of a deep alluvium layer derived from the surrounding mountain flanks, with additional formations including limestones and granites. Elevation ranges from lower desert elevations of 1250 meters up to the Whetstone Pediment at 1585 meters above sea level (Southwest Watershed Research Center, 2003). The Whetstone Pediment slopes westward from the Dragoon Mountains, whose western flank provides runoff input to Walnut Gulch’s ephemeral stream network. The Dragoons partially compose the WGEW; specifically, the northern and central portions of the mountain range form part of the eastern boundary, acting as transition zone between the Sonoran and Chihuahuan Desert.

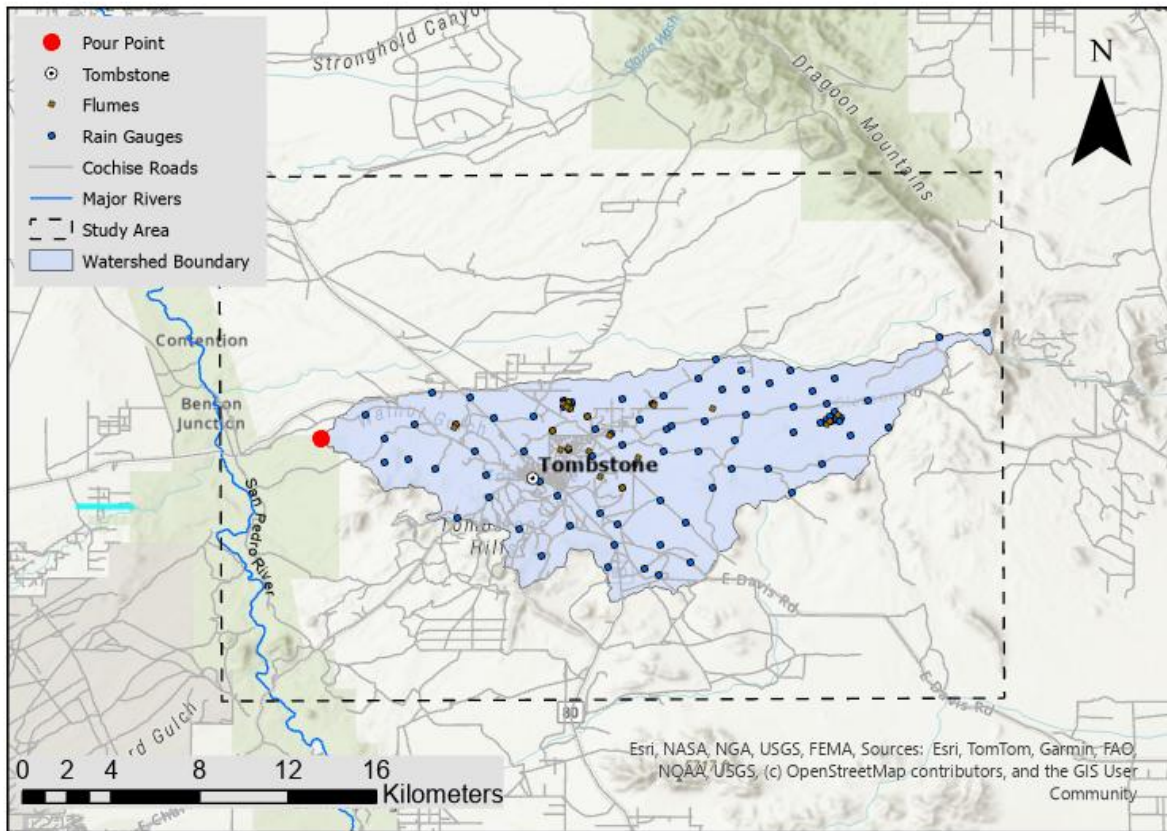


Figure 1. Study area includes the Walnut Gulch Experimental Watershed, situated near Tombstone, Arizona, USA—bounded to the west by the San Pedro River and to the east by the Dragoon Mountains.

Vegetation across the watershed consists mostly of shrubs in the lower region and grasses in the upper region. WGEW is contained within 60 million hectares of rangeland used primarily for cattle grazing in southwestern U.S. (Southwest Watershed Research Center, 2003). The climate of the WGEW is classified as semi-arid. The mean annual temperature at Tombstone is 63.9 °F, with an average of 350 mm of annual precipitation. Most of the precipitation occurs during the North American Monsoon season, which begins in July and ends in September. These high-intensity convective thunderstorms generate rapid hydrologic responses with variable runoff peaks over

short durations. Winter precipitation, driven by slower-moving frontal systems, contributes minimal streamflow.

Observed by the Southwest Watershed Research Center (SWRC), WGEW serves as a long-term outdoor laboratory for hydrological, erosion, and climate-related research in rangeland ecosystems. The USDA Agricultural Research Service selected the watershed in the mid-1950s as a research facility to develop technology for quantifying how upland conservation practices impact downstream water supply. Watershed instrumentation consists of numerous rain gauges, flumes, soil moisture sensors, stock ponds, and meteorological stations. These facilities enable detailed monitoring of precipitation, runoff, sediment transport, and evapotranspiration processes, generating large datasets that have supported the development and validation of hydrologic models including CREAMS, RUSLE, WEPP, KINEROS, EPIC, SPUR, and CLIMATE (Southwest Watershed Research Center, 2003).

Data

This study utilized four primary spatial datasets to support NDII-based infiltration analysis and erosion control suitability modeling within the WGEW. All datasets were mapped to illustrate spatial extent and characteristics, and metadata tables are provided in the appendix. Each dataset is described below.

1. Shuttle Radar Topography Mission (SRTM) 1 Arc-Second Global DEM

The SRTM 1 Arc-Second Global dataset (Table A1) was sourced from USGS EarthExplorer. It provides a 30-meter resolution digital elevation model derived from radar interferometry aboard the Space Shuttle Endeavour. This DEM was used to delineate watershed boundaries, calculate slope, and support hydrological modeling. The data are void-filled and referenced to WGS84 horizontal and EGM96 vertical

datums. Two adjacent tiles were merged to fully cover the WGEW area, and the final raster was clipped to the study area.

2. Landsat 8–9 OLI/TIRS Collection 2 Level-2 Surface Reflectance Imagery

Landsat imagery was obtained from USGS EarthExplorer (Table A2). Four scenes spanning 2020 and 2022 were selected to capture seasonal NDII dynamics. The Level-2 products include atmospherically corrected surface reflectance bands with a spatial resolution of 30 meters, which were used to compute NDII and assess temporal changes in soil moisture.

3. SWRC Flume and Rain Gauge Locations

Flume and rain gauge locations were sourced from the SWRC ArcGIS Hub (Table A3). This dataset includes georeferenced point features representing instrumentation across WGEW. These locations were used to validate NDII trends and prioritize zones for erosion control based on proximity to monitored catchments. The dataset includes metadata on flume type, operational years, and elevation, which were integrated into the suitability analysis.

4. Arizona Rivers Layer from ArcGIS Online

Hydrographic features were extracted from the Arizona GIS Portal (Table A4). This dataset provided the location of the San Pedro River for orientation purposes.

5. Primary and Secondary Roads Dataset (TIGER/Line 2024)

The shapefile was sourced from the U.S. Census Bureau TIGER/Line archive (Table A5). It includes vector line features for all roadways in Cochise County, Arizona, used to assess accessibility in multi-criteria suitability modeling. This dataset is projected in NAD83 and supports proximity scoring.

6. Rain Gauge Data (Tucson ARS Aggregate Portal)

Rainfall data were downloaded from the USDA ARS Tucson Digital Aggregate Portal, which provides long-term precipitation records from digital gauges across the WGEW (Table A6). Users can select specific gauges and time intervals to generate aggregated statistics such as mean, maximum, and standard deviation. Data are available in multiple formats (HTML, Excel, text) and support temporal analysis of rainfall variability. These records were used to identify driest and wettest years, validate NDII-derived infiltration trends and assess hydrological response during dry and wet seasons. The dataset is updated regularly and includes metadata on gauge locations, watershed affiliation, and measurement intervals.

Data Processing

Summary

This study employs a three-part methodology encompassing precipitation analysis, remote sensing, and terrain evaluation (Figure 2). Precipitation analysis identifies the driest and wettest years to frame the temporal scope of the study. Remote sensing analysis generates NDII pattern change rasters to detect zones of low infiltration. Terrain analysis delineates watershed boundaries and performs suitability modeling to prioritize ORD installation zones. Finally, a validation model is applied to assess the correlation between rain gauge data and NDII values within identified priority zones.

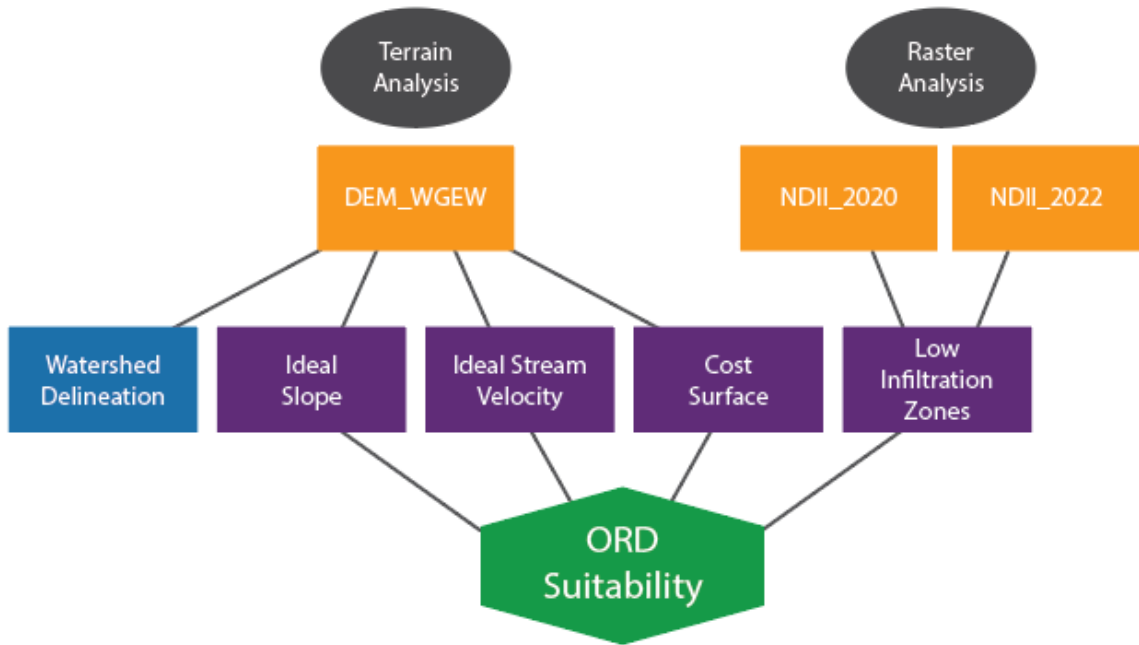


Figure 2. Methodology summary of analysis for ORD placement suitability.

Precipitation Analysis

Precipitation data from the Southwest Watershed Research Center (SWRC) were accessed via its digital archive, which includes core monitoring network measurements in analog format up to 1999 and digital format from 2000 onward. An Excel spreadsheet of aggregate annual rainfall totals (Figure 3) was used to calculate average precipitation across gauges in the WGEW. Based on these values, 2020 was identified as the driest year (8.71 centimeters) and 2022 as the wettest (37.90 centimeters) between 2015 and 2025. These precipitation extremes informed the selection of Landsat 8/9 imagery for NDII analysis, enabling comparison of soil moisture signals between dry and wet hydrological conditions.

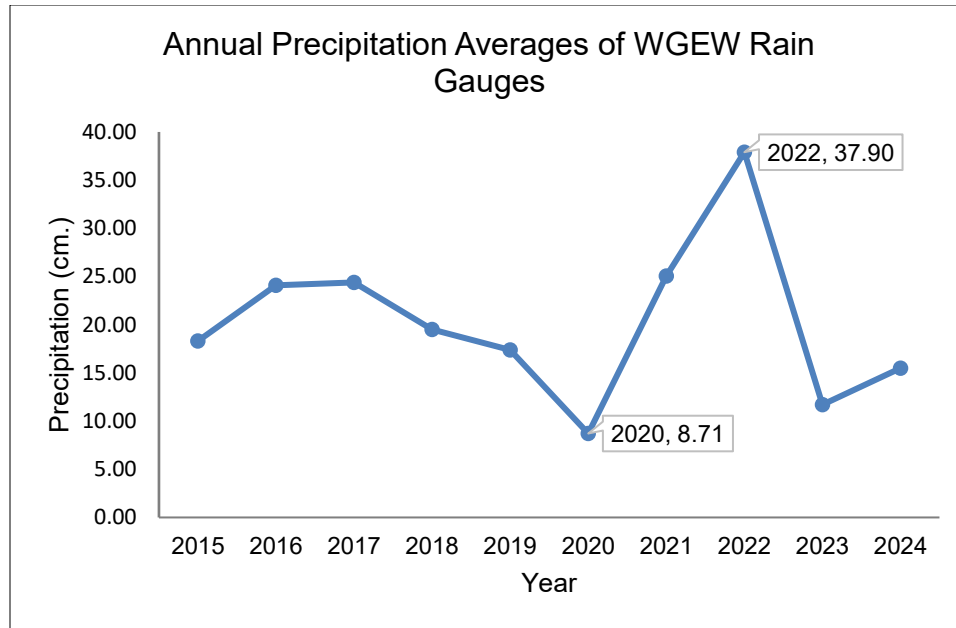


Figure 3. Total annual precipitation (in centimeters) derived by averaging aggregate rain gauge measurements across all stations for each calendar year. These values were used to identify the driest and wettest years included in the NDII analysis.

Landsat Imagery Collection

Using Earth Explorer, Landsat 8 and 9 scenes for the pre- and post-monsoon seasons of the driest and wettest years were selected with 0% cloud coverage on path 035 and row 038. Since the monsoon season typically spans July through September, scenes from May and October were used to capture conditions before and after seasonal rainfall. Calculating NDII change between these intervals allows for the identification of spatial variations in soil moisture dynamics driven by infiltration. NDII is sensitive to changes in vegetation water content, which has been shown to closely correlate with root zone moisture, particularly during periods of hydrological stress (Sriwongsitanon et al., 2016). This comparison helps distinguish areas with consistent low infiltration or recovering moisture conditions—critical inputs for suitability modeling in erosion control planning.

R Script Analysis

NDII Analysis

Four cloud-free Landsat 8 and 9 scenes spanning pre- and post-monsoon periods for 2020 and 2022 were downloaded from EarthExplorer (path 035, row 038). Each scene was processed using the terra package in R. Reflectance bands were stacked and saved as multi-band raster files to facilitate NDII calculation.

Hardisky et al. developed NDII in 1983; computed using band 5 (NIR) and band 6 (SWIR), with NDII defined as:

$$NDII = \frac{NIR - SWIR}{NIR + SWIR}$$

This index, sensitive to vegetation water content, serves as a proxy for root zone moisture dynamics. NDII rasters were computed for all four scenes, and image alignment was achieved using bilinear resampling to prepare rasters for differencing.

NDII change maps were generated for 2020 and 2022 by subtracting pre-monsoon NDII from post-monsoon NDII capturing the seasonal moisture gain or loss attributed to infiltration. Each change map was then reclassified into five infiltration categories:

Strong Decrease (≤ -0.2)

Moderate Decrease (-0.2 to -0.05)

Stable (-0.05 to 0.05)

Moderate Increase (0.05 to 0.2)

Strong Increase (> 0.2)

Reclassified rasters were exported for integration into suitability modeling frameworks.

Digital Elevation Model Preparation

To support elevation-derived suitability factors such as slope and stream delineation, Shuttle Radar Topography Mission (SRTM) tiles (n31_w110, n31_w111) were merged into a seamless digital elevation model (DEM) covering the WGEW, using R. This merged DEM was exported as GeoTIFF and imported into ArcGIS Pro for spatial analysis.

ArcGIS Model Builder

This project used ArcGIS ModelBuilder to identify priority zones for ORD placement in Walnut Gulch. The workflow included watershed delineation with a refined pour point, terrain analysis using slope and flow accumulation, and stream velocity modeling via the Maidment et al. (1996) slope–area method. A cost surface was developed from road proximity and ruggedness. NDII change rasters were reclassified to isolate low-infiltration zones. All inputs—ideal slope, velocity, infiltration stress, and cost surface (≤ 2.5)—were merged to create a final suitability raster. Figure 4 illustrates the integrated steps guiding ORD prioritization.

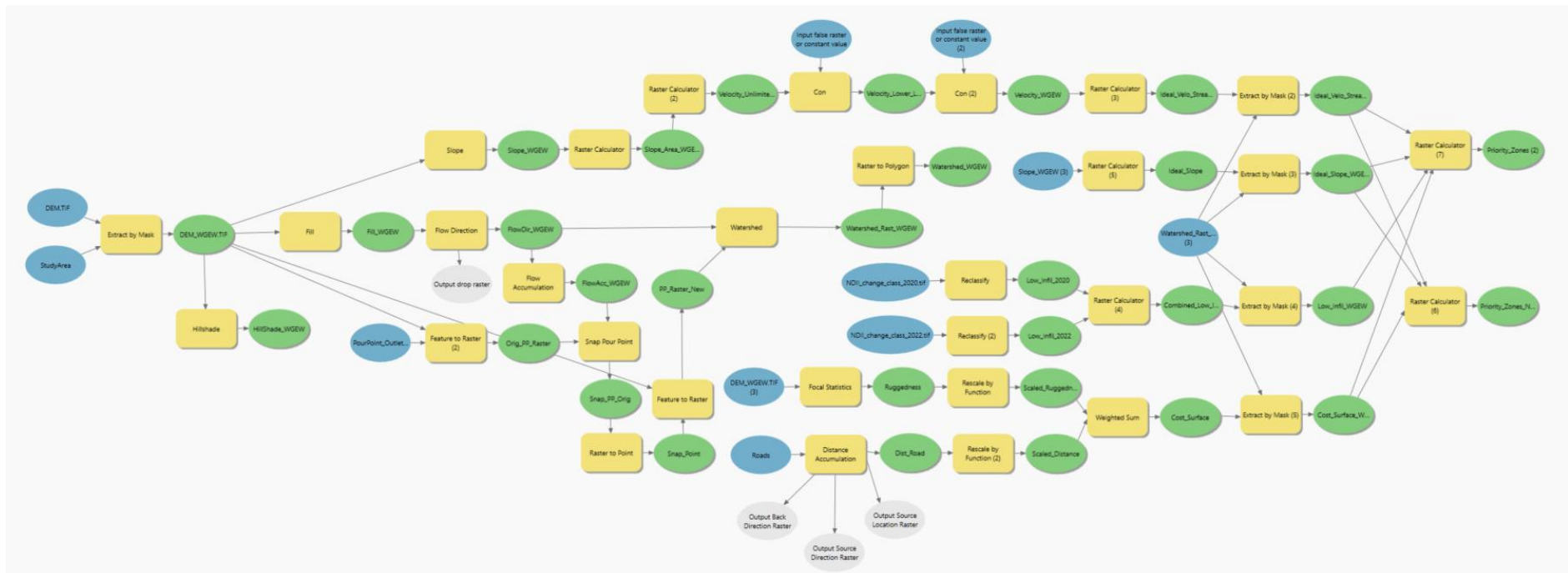


Figure 4. Workflow constructed in ArcGIS Pro ModelBuilder illustrating the automated sequence for hydrological and suitability analysis within the WGEW.

Watershed Delineation

The pour point for the WGEW was placed at the outlet flume at 31°43'45.3"N, 110°9'12.1"W (decimal: 31.72925°, -110.15336°), east of the San Pedro River, outside Tombstone, Arizona. This location serves as the terminal monitoring site for runoff and is commonly used as the downstream reference in hydrological modeling workflows (University Corporation for Atmospheric Research, n.d.). After digitizing this location and converting into raster format—matched to the resolution and extent of the clipped DEM—the pour point raster was integrated into the watershed delineation process. This enabled accurate upstream catchment mapping using ArcGIS Pro's *Watershed* tool, anchored to this known hydrological outlet.

To delineate the watershed in ArcGIS Pro, the clipped DEM was first processed using the *Fill* tool to remove localized depressions or “sinks”— caused by resolution errors or rounded elevations. This preprocessing step ensures proper hydrologic continuity and accurate flow routing across the terrain surface. Next, the *Flow Direction* tool was applied to the filled DEM using the D8 algorithm, which assigns each cell a direction based on the steepest downslope among its eight neighbors. This raster provides the directional framework for downstream flow analysis.

Building on the flow direction output, the number of upstream cells contributing flow to each cell in the DEM were quantified (*Flow Accumulation tool*), thereby identifying drainage paths and channel networks. To ensure alignment between the outlet point and these flow paths, the *Snap Pour Point* tool repositioned the user-defined pour point to the nearest high-flow cell within a specified threshold. However, due to the relatively flat terrain near the pour point, flow accumulation values differed only marginally across the area, resulting in the snapped pour point relocating to the eastern

edge of the study window—where values were minimally higher. This led to a misaligned watershed polygon that deviated from the published boundaries of the WGEW, particularly along the western margin. To correct this discrepancy, the snapped pour point was manually placed on a nearby high-flow cell that better represents the true outlet. These refined inputs were then used to generate the final polygon (Figure 5) representing the contributing area upstream of the pour point (*Watershed tool*). This workflow produced a hydrologically consistent watershed boundary suitable for subsequent analysis.

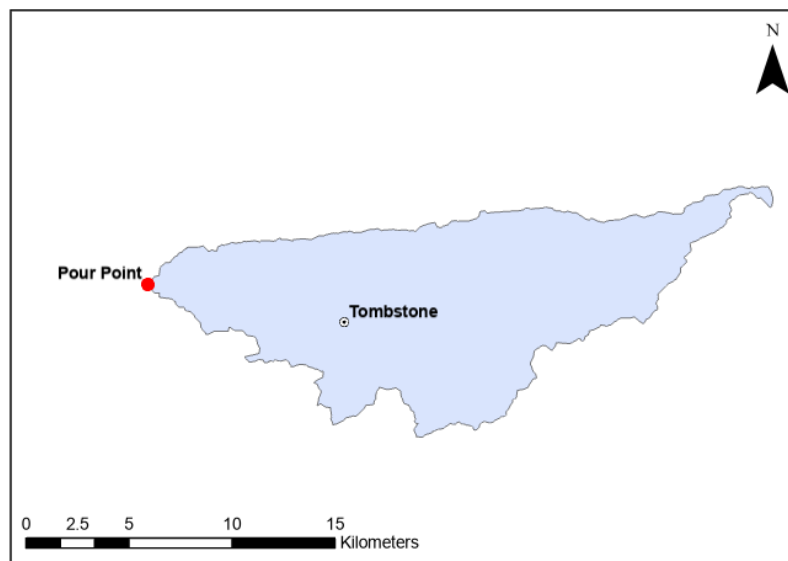


Figure 5. Hydrologically derived polygon showing the final watershed boundary delineation for WGEW.

Cost Surface Development

Assessing accessibility metrics is a critical component in evaluating the feasibility of installing ORD structures for restoration purposes. As emphasized by Maestas et al. (2018), accessibility was among the primary criteria used to narrow down suitable

project sites. Accessibility encompasses both proximity to roads and terrain ruggedness, recognizing the logistical challenges of manual installation.

Accessibility to potential ORD installation sites was modeled using a weighted cost surface derived from road proximity and terrain ruggedness. The *Distance Accumulation* tool generated a raster of travel cost from roads using a road network shapefile, simulating field access effort under supply-limited conditions. Ruggedness was quantified using the study area's DEM, calculating elevation range within neighborhood cells to represent terrain variability (*Focal Statistics tool*). Both outputs were rescaled to a uniform range of 1 to 10 (*Rescale by Function tool*), to facilitate a cost surface. The cost surface was calculated by assigning a higher weight (1.25) to road distance and a standard weight (1.0) to ruggedness (*Weighted Sum tool*), reflecting the practical importance of resupply access over modest terrain variation.

Slope and Velocity Suitability Criteria

To ensure the long-term effectiveness of ORDs, careful consideration of site conditions—particularly slope and stream velocity—is essential. These factors influence both structural longevity and the likelihood of avoiding unintended channel degradation due to misplacement. Ecologist Alan Hayden, speaking at a U.S. Geological Survey conference, emphasized that although ORDs are simple in form, their success relies on thoughtful design that accounts for geomorphology and hydrology (U.S. Geological Survey, 2024). Each structure alters the energy dynamics within the stream, reinforcing the need to evaluate sediment load, discharge variability, and local channel evolution. Channel recovery is facilitated through ORD placement, as each structure slows streamflow, promotes sediment deposition, and fosters vegetation establishment—processes that can progressively raise incised channel beds (Maestas et al., 2018). In

our strategy, we targeted low to moderate-gradient ephemeral and intermittent streams and a stream velocity threshold to promote stability and minimize failure risk.

A terrain slope range of 2% to 4% was selected as an optimal window for ORD installation. This selection aligns with guidance from Zeedyk et al. (2018), who recommend ORD placement in low-gradient (<3%) intermittent or ephemeral drainages to promote infiltration and channel recovery. Slopes below 2% were excluded to avoid pooling or stagnation that could compromise the structure's effectiveness and vegetation health. To delineate these areas, the *Slope* tool was applied to the DEM, generating a raster of terrain variability. The *Raster Calculator* tool was used to isolate cells within the 2% to 4% range, forming a suitability mask for ORD placement.

Stream velocity was modeled using a slope–area approach proposed by Maidment et al. (1996), as implemented in the ArcGIS Learn tutorial by Esri (n.d.) (*Raster Calculator tool*).

The slope-area term (S^bA^c) was calculated:

$$\text{Slope Area Term} = \sqrt{\text{Slope}} * \sqrt{\text{Flow_Accumulation}}$$

This reflects the recommended values for b and c of 0.5, equivalent to the square root.

Velocity was then computed using Maidment et. Al (1996) equation (*Raster Calculator tool*):

$$\text{Velocity} = \text{Velocity Average} * \frac{\text{Slope Area Term}}{\text{Slope Area Term Average}}$$

Where the slope area term average was derived from raster statistics (mean = 8.1417), and Velocity average was assumed to be 0.1 m/s, appropriate for ephemeral channels targeted in this study.

To remove unrealistic velocity extremes, thresholds were applied using the *Con* tool, isolating values over .2 m/s and under 2 m/s for further modeling; cells with values greater than .2 m/s were isolated (*Raster Calculator tool*) for the ideal velocity mask.

NDII Reclassification for Infiltration Zones

The imported NDII change classification rasters were reclassified to distinguish suitable versus non-suitable areas for erosion control intervention. Using the *Reclassify* tool, zones previously categorized as Strong Decrease (≤ -0.2), Moderate Decrease (-0.2 to -0.05), and Stable (-0.05 to 0.05) were considered suitable for ORD placement, as these areas exhibited persistently low infiltration and would benefit from hydrological restoration. This classification approach aligns with findings from Sriwongsitanon et al. (2016), who demonstrated that NDII is a reliable proxy for root zone moisture deficit, particularly during periods of water stress. To identify consistently low infiltration zones across both dry and wet seasons, a conditional expression combined common moisture stress zones (*Raster Calculator tool*). This produced a composite layer highlighting areas that met the low infiltration criteria in both years, serving as a foundation for ORD prioritization.

Final Suitability Raster and Prioritization Zones

A comprehensive suitability assessment was performed by integrating all key raster inputs: cost surface, ideal slope, ideal stream velocity, and combined low infiltration layers. Each raster was clipped to the WGEW boundary to ensure spatial consistency and relevance to hydrological restoration targets.

To generate the final suitability raster, the following expression was entered into the *Raster Calculator* tool:

$$\text{Ideal Velocity} * \text{Ideal Slope} * \text{Combined Low Infiltration} * (\text{Cost Surface} \leq 2.5)$$

The cost surface was limited to values ≤ 2.5 to represent zones with optimal field accessibility and minimized implementation constraints. This filtering refined the prioritization output to highlight areas where physical terrain, hydrological stress, and feasibility converge, enabling focused ORD placement in corridors most likely to benefit from grade control and infiltration enhancement.

For comparative purposes, the same procedure was repeated excluding the low infiltration layer, allowing evaluation of how NDII-informed zones influence prioritization outcomes relative to terrain-only criteria.

Validation Methods

To validate NDII-derived priority zones for erosion control, a spatial and temporal comparison was conducted between seasonal NDII change values and rain gauge precipitation totals across the WGEW. Using ArcGIS Model Builder, a new workflow (Figure 6) linked NDII stress signals with observed rainfall data to assess whether flagged low-infiltration zones correspond to hydrological deficits or runoff-dominated behaviors.

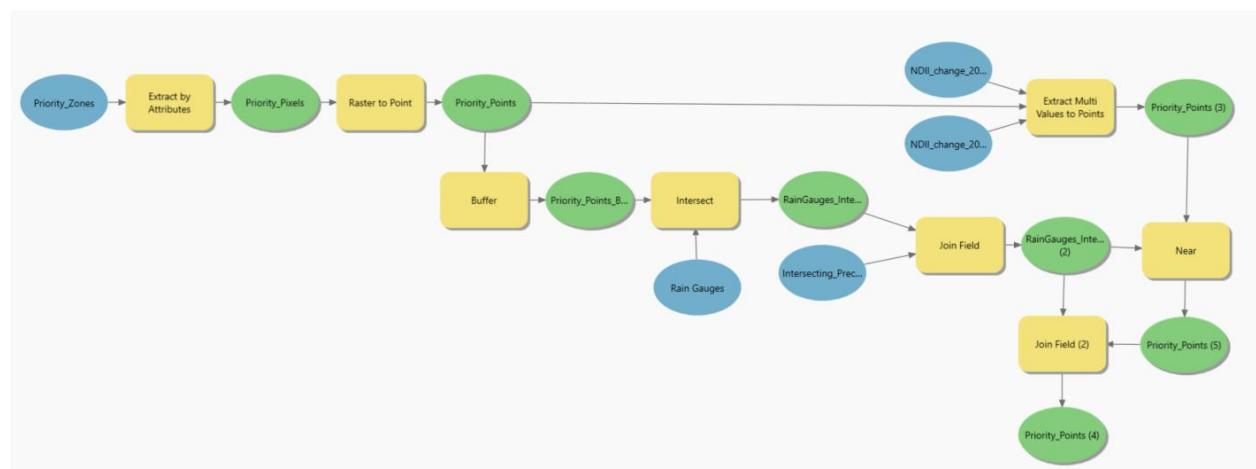


Figure 6. Validation model illustrating the spatial and statistical workflow used to assess the effectiveness of NDII as a proxy for identifying low-infiltration zones within the WGEW.

Priority Zone Extraction

Priority zones identified in the final suitability raster were first extracted using the *Extract by Attributes* tool, isolating cells flagged for erosion control intervention. These raster pixels were converted to point features (*Raster to Point tool*), generating a shapefile of NDII-prioritized locations across WGEW.

NDII Value Extraction

NDII change maps-developed during the NDII analysis scripting in R-representing change from pre- and post-monsoon NDII values for 2020 and 2022 were processed to extract pixel-level values at each priority point. Using the *Extract Multi Values to Points* tool, NDII change values for both years were appended to the priority points table, enabling comparison of soil moisture response across contrasting rainfall conditions.

Rain Gauge Association

To establish spatial relationships between rain gauges and priority zones, a 1000-meter buffer was applied around each priority point (*Buffer tool*, Figure 7). The 1000-meter distance was selected to reliably capture nearby rainfall data while maintaining spatial relevance to each priority point. These buffered zones were intersected with the SWRC rain gauge layer (*Intersect tool*), isolating gauges within proximity to NDII-prioritized locations. Annual aggregate precipitation totals for 2020 and 2022, were joined to the intersected gauges table (*Join Field tool*). Using the *Near Tool*, the closest rain gauge was established ensuring rainfall totals were directly associated with each NDII zone.

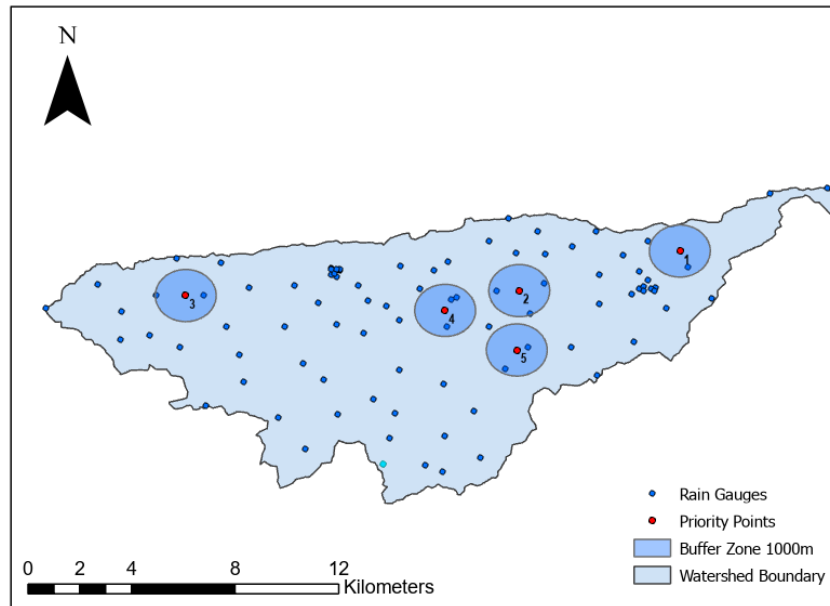


Figure 7. Spatial visualization of 1000-meter buffer zones surrounding NDII-prioritized erosion control points used to identify nearby rain gauges for precipitation comparison and validation.

Integrated Comparison

The final validation dataset included each priority point's NDII change values, associated rain gauge ID, precipitation totals for 2020 and 2022, and the spatial distance to the nearest gauge. This dataset enabled correlation analysis and visual comparison of infiltration behavior under varying hydrological inputs.

RESULTS

Composite Suitability for ORD Placement in WGEW

Seasonal NDII Variation and Infiltration Patterns

To quantify spatial and seasonal variation in soil moisture, NDII rasters were generated via R scripting for both 2020 and 2022 (Figure 8). Seasonal change was assessed by subtracting pre-monsoon NDII values from post-monsoon measurements, and results were classified into five categories: Strong Decrease (≤ -0.2), Moderate Decrease (-0.2 to -0.05), Stable (-0.05 to 0.05), Moderate Increase (0.05 to 0.2) and Strong Increase (> 0.2). In 2020, the driest year of the past decade with total average annual precipitation of 8.71 centimeters, NDII values predominantly exhibited moderate increases across the study area. Low antecedent soil moisture resulted in higher infiltration potential, whereby even minimal post-monsoon precipitation significantly elevated root-zone water content. This aligns with findings from Sriwongsitanon et al. (2016), which indicate NDII's sensitivity to suction pressure in the root zone and “the correlation is strong during periods of moisture stress, but that when the root zone is near saturation the correlation is weak.” (p.14). Conversely, 2022—characterized by high annual rainfall average (37.90 centimeters)—showed predominantly stable NDII patterns. Saturated soil conditions prior to the monsoon limited additional infiltration, resulting in minimal seasonal NDII. These contrasting patterns demonstrate NDII’s utility in detecting plant stress responses and short-term hydrological shifts in semi-arid environments. By extracting pixels classified as ‘Stable’, ‘Moderate Decrease’, and ‘Strong Decrease’ from both NDII rasters, a conditional composite can be used to

identify common zones of consistently low infiltration despite annual variability in precipitation.

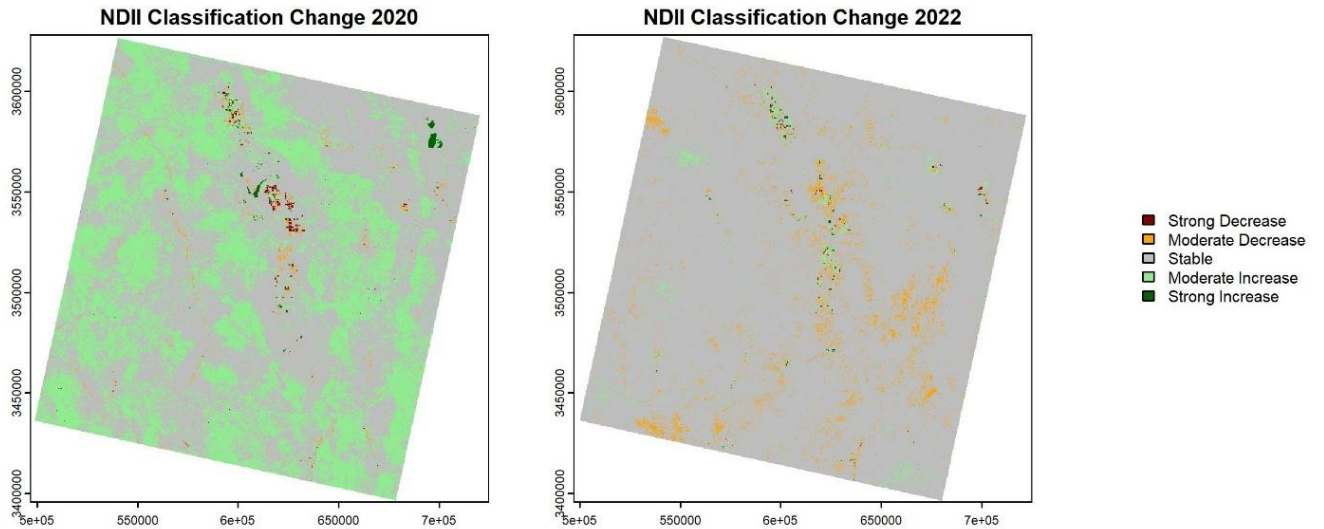


Figure 8. Annual rasters depicting NDII-based classification changes derived from seasonal comparisons between pre- and post-monsoon periods.

Since most of the cells within the WGEW boundary remained within the stable classification (Figure 9), they were included in the suitability analysis. In semi-arid environments, such stability—particularly in NDII-derived moisture indices—often reflects persistently dry conditions and limited hydrologic variability. Including these cells is crucial for three reasons: (1) they provide a baseline against which temporal anomalies can be detected, (2) they help validate assumptions about long-term moisture stress and vegetation sparsity, and (3) they allow the identification of chronically dry zones that may be more prone to erosion due to reduced canopy cover and poor infiltration. Dry zones tend to exhibit greater spatial variability in soil moisture

compared to wetter regions. This pattern aligns with findings by Korres et al. (2015), who observed a negative correlation between the coefficient of variation and mean soil moisture across multiple datasets, indicating lower variability at higher moisture levels. Ultimately, stability in this context strengthens the case for targeted restoration interventions by highlighting areas where low-moisture conditions persist regardless of seasonal rainfall.

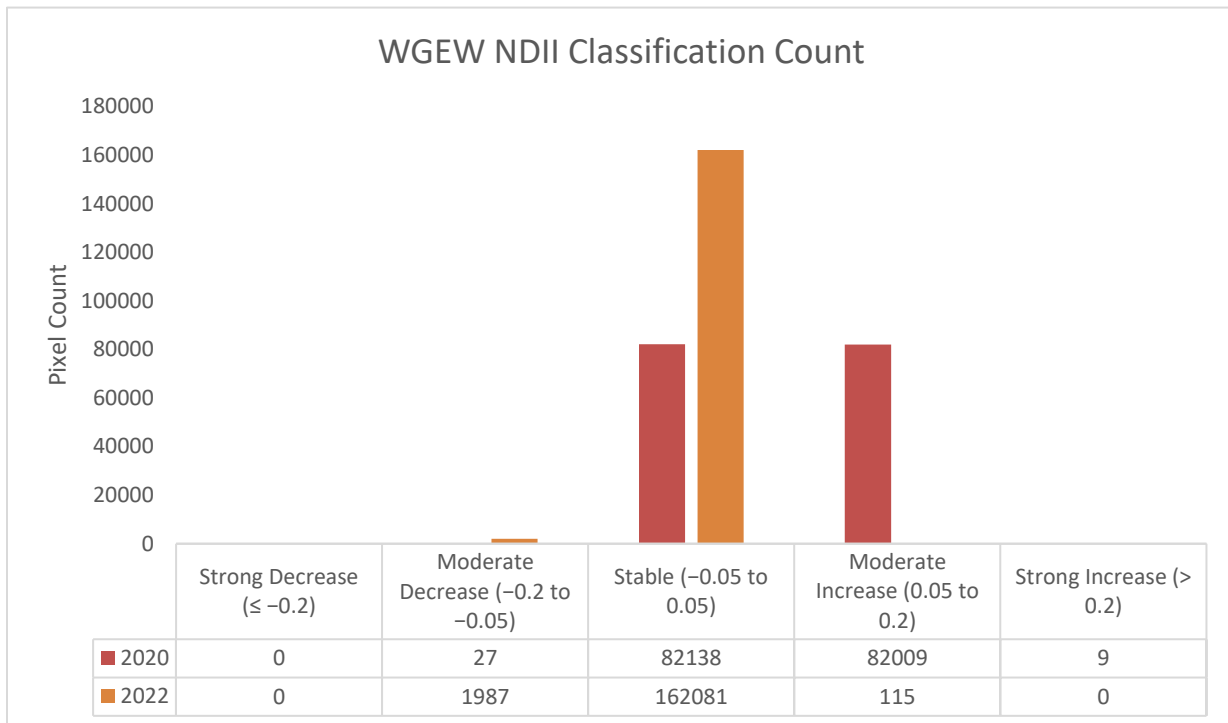


Figure 9. Distribution of NDII Classification Categories Within the WGEW from 2020 to 2022. The predominance of stable classifications reflects persistently dry conditions across much of the watershed and underscores the limited hydrologic response typical of semi-arid environments.

Areas exhibiting consistently low infiltration—indicated by persistently low soil moisture across both years—were combined to inform the final suitability analysis. This approach identified 72.99 hectares (811 pixels) within the WGEW boundary (Figure 10), representing chronically low-infiltration zones prioritized for targeted restoration efforts.

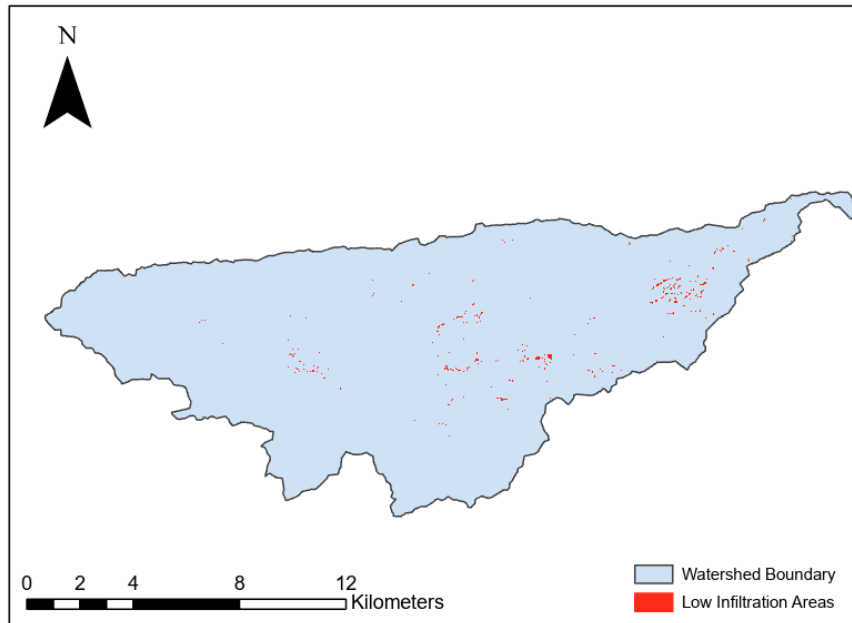


Figure 10. Low infiltration zones identified through NDII analysis, based on combined 2020 and 2022 rasters where values consistently remained within or below stability thresholds.

Logistical Accessibility: Ruggedness and Road Proximity Analysis

To quantify accessibility, a cost surface analysis (Figure 11) identified areas requiring less manpower for access, thereby distinguishing feasible zones from more remote and labor-intensive regions. Given that WGEW is situated on an alluvial fan, terrain ruggedness is generally minimal, with greater roughness observed only in the southwestern sector. As a result, proximity to roads emerged as the dominant accessibility factor. The western portion of the watershed features denser road networks than the eastern side, which is comparatively under-connected. Overall, the watershed demonstrates high logistical suitability, with most zones readily accessible for field operations.

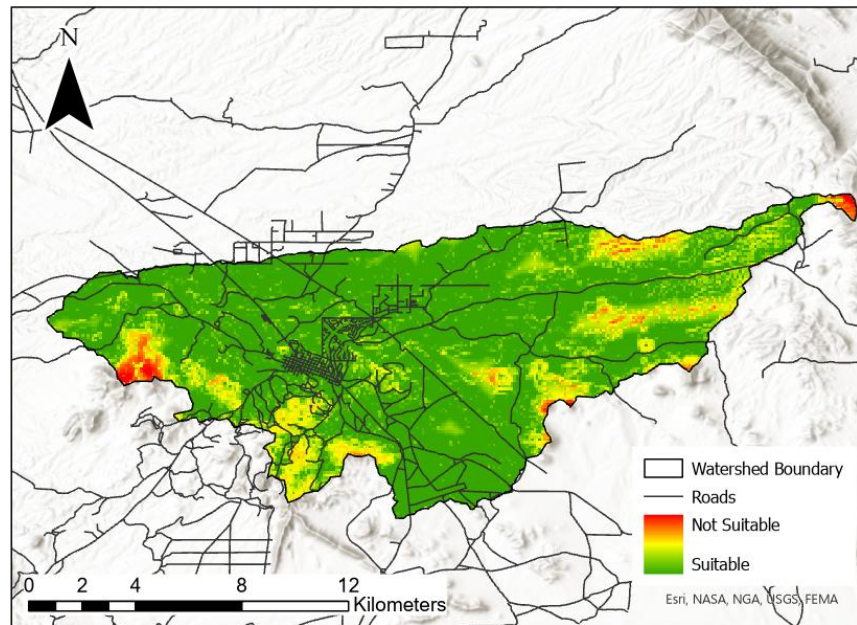


Figure 11. Cost surface raster depicting suitable areas (green) with favorable accessibility based on terrain ruggedness and proximity to road networks.

Geomorphic Parameters for ORD Suitability

Ideal slope and stream velocity conditions are essential for the longevity and effectiveness of ECS. Proper placement supports stream stability and ecological resilience, while misplacement may exacerbate erosion or disrupt channel flow. In this study, ORDs are prioritized for their grade control functionality and suitability in low- to moderate-gradient channels.

Slope analysis identified 3,174.60 hectares (35,273 pixels) that fall within the target gradient range of 2% to 4%, representing areas suitable for ORD installation (Figure 12). These low slopes support sediment deposition without overwhelming the structural integrity of the dam. Placement within these zones reduces erosion potential and enhances the structure’s lifespan by aligning with natural flow dynamics.

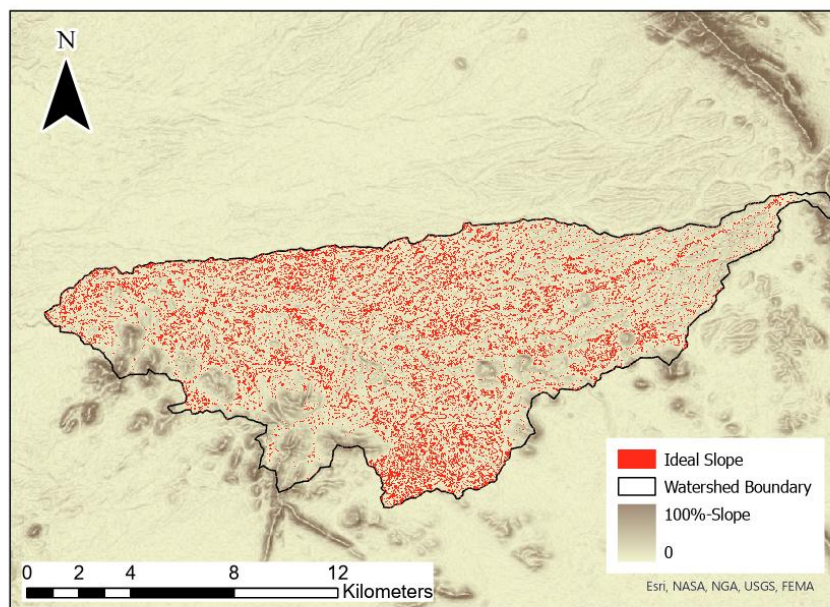


Figure 12. Ideal slope raster identifying zones with gradients between 2% and 4% across the WGEW, suitable for one rock dam placement.

Stream velocity analysis further refined the suitability framework by isolating ephemeral and intermittent stream segments (1,297.20 hectares, 14,413 pixels) exhibiting flow rates between 0.2 m/s and 2 m/s. Within this range, energy levels remain low enough to prevent scouring or excessive pool formation downstream of the ORD. Mapping these segments (Figure 13) provides an additional layer of precision in targeting restoration zones, ensuring that each installation contributes to long-term channel stability and sediment retention.

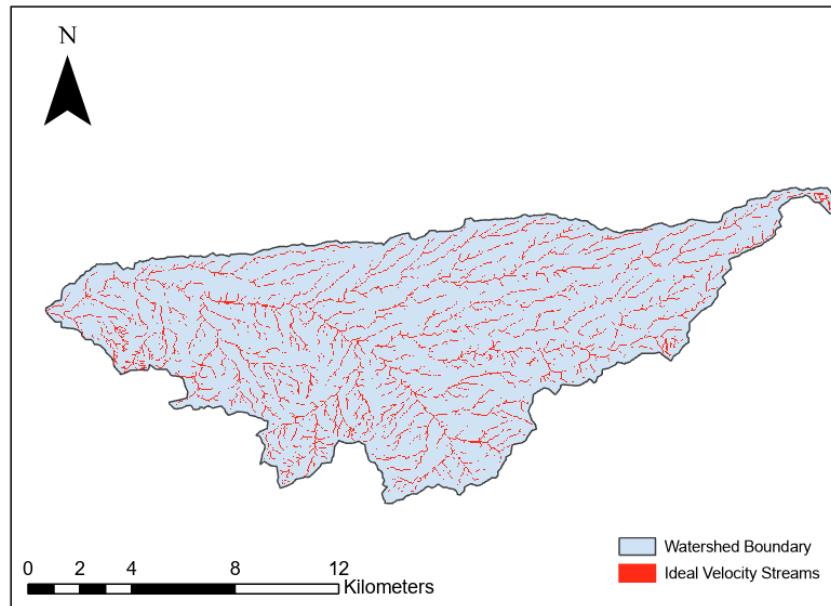


Figure 13. Stream velocity raster highlighting ideal segments within the WGEW where flow rates range between 0.2 m/s and 2.0 m/s, suitable for erosion control structure placement.

Composite Suitability Zones for ORD Installation

Combining all four variables—ideal velocity, ideal slope, cost surface, and combined low infiltration—yielded five suitable ORD locations (Figure 14). Notably, four of these sites are on the eastern half of WGEW on streams fed by the upper watershed, aligning with recommendations by Cuenca Los Ojos, Borderlands Restoration Network, and the Biophilia Foundation (2021), who emphasize positioning ORDs higher in the watershed to enhance infiltration and water retention.

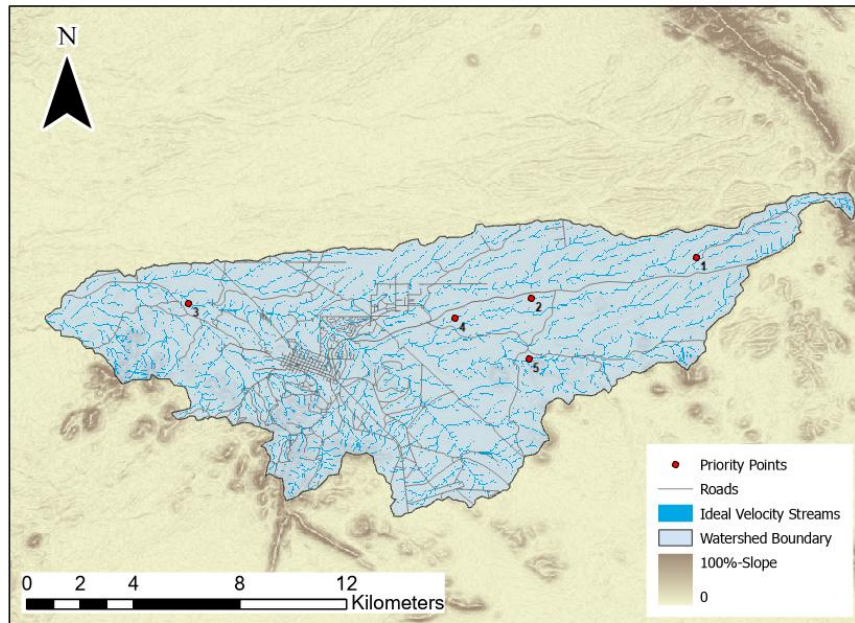


Figure 14. Composite suitability raster identifying high-priority points for ORD placement within WGEW, derived from slope, stream velocity, soil moisture, and accessibility metrics.

Incorporating NDII, as a proxy for low infiltration zones, significantly reduced the number of suitable locations for ORD locations compared to the terrain-based suitability analysis (Figure 15). While NDII integration identified five high-priority sites, the broader approach yielded 454 potential locations. This refined output is not without tradeoffs. Reducing the number of candidate sites could constrain redundancy and adaptability, especially if the chosen zones fail to perform as expected due to unpredictable soil or climate conditions. To mitigate the risks associated with reduced flexibility, these five sites are proposed as primary candidates for pilot implementation. Targeting these five sites and evaluating their effectiveness offers a practical and scalable path forward. These priority sites can serve as focal zones for deploying multiple ORDs in proximity,

enhancing implementation success. This focused assessment of infiltration potential demonstrates NDII's utility in narrowing candidate zones to those most ecologically suitable.

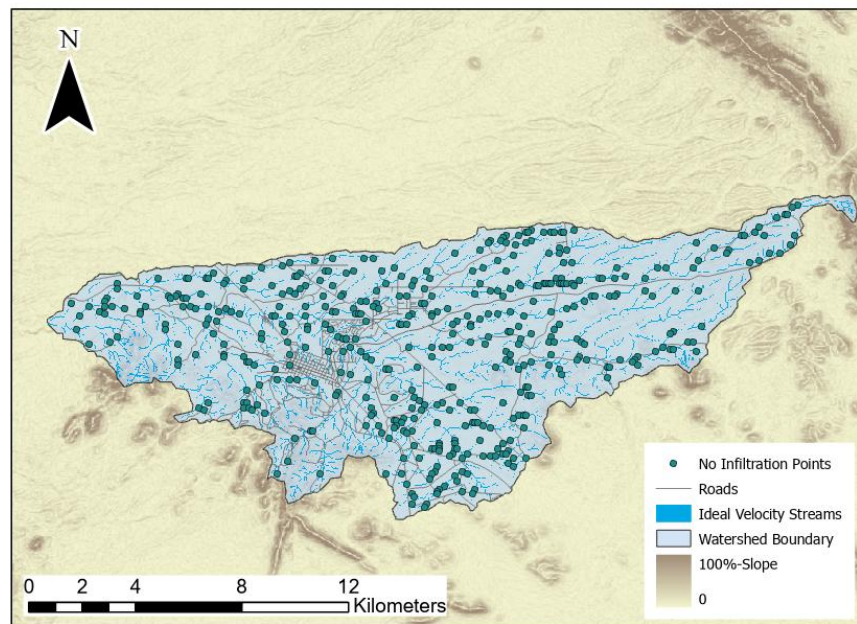


Figure 15. Terrain-based priority zone raster for ORD placement within the WGEW excluding low infiltration zones and focusing solely on slope, ruggedness, and accessibility criteria.

NDII-Based Moisture Validation Using Rain Gauge Data

A spatial and temporal comparison of seasonal NDII changes and rain gauge-derived annual precipitation averages revealed NDII values are most useful at identifying low infiltration zones during periods of drought versus saturated periods. This is consistent with Sriwongsitanon et al. (2016), who emphasized NDII's utility during moisture stress periods. As shown in Table 1, NDII values were positive during the 2020 season—a season marked by lower rainfall—signaling preexisting heightened

vegetation stress was more susceptible to a positive change even at low precipitation. In contrast, the 2022 season exhibited negative NDII values during higher precipitation periods, suggesting saturated soil moisture and vegetation recovery. These findings affirm NDII's utility as a dynamic proxy for surface moisture variability, particularly in semi-arid watersheds such as WGEW, and provide a critical lens for prioritizing ORD sites during stress-prone intervals and less effective during periods of heavier precipitation. Utilizing NDII during dry seasons enhances the detection of areas with limited infiltration, offering more effective insights for moisture-stress analysis and effective restoration planning.

Priority Point	Rain Gauge	Gauge Dist. (m)	2020		2022	
			NDII	Precip. (cm.)	NDII	Precip. (cm.)
1	wg_rg065	666.34	0.035	7.65	-0.0520	49.43
2	wg_rg044	762.78	0.042	5.61	-0.0636	40.67
3	wg_rg012	591.01	0.046	9.88	-0.0564	40.18
4	wg_rg039	445.07	0.037	4.60	-0.0507	35.81
5	wg_rg053	379.10	0.041	6.65	-0.0512	38.18

Table 1. Data table summarizing joined attributes for NDII-prioritized points. Each row represents a priority location linked to its nearest rain gauge, including NDII change values for 2020 and 2022, rain gauge ID, spatial distance to the gauge (in meters), and aggregate annual precipitation totals (in centimeters).

CONCLUSION

Summary

This study highlights the efficacy of normalized difference infrared index as a strategic proxy for identifying infiltration patterns and erosion control suitability within the Walnut Gulch Experimental Watershed, emphasizing zones that remained persistently dry despite contrasting precipitation years. By integrating remote sensing indices, hydrologic velocity, terrain variability, and accessibility analysis, the study successfully identified five high-priority locations for one rock dam placement—highlighting the power of gauge-independent, data-driven restoration frameworks. This strategic framework pursued two primary objectives designed to assess NDII's utility in watershed restoration planning.

Study Objectives & Outcomes

(1) Can NDII be used to identify zones with low soil moisture and high suitability for ORD placement?

NDII proved highly effective in identifying chronically dry zones across WGEW. The dominance of stable NDII classifications across both dry (2020) and wet (2022) years suggested persistently low moisture and minimal seasonal hydrological response. By isolating pixels within the 'Stable', 'Moderate Decrease', and 'Strong Decrease' categories, the analysis pinpointed 811 locations with sustained infiltration stress. These were prioritized for ORD installation. NDII functioned not only as a proxy for soil moisture but also as a strategic filter in multi-criteria suitability modeling.

(2) Do NDII trends at identified zones correlate with precipitation data collected from rain gauges?

A clear inverse correlation emerged between NDII change values and annual average precipitation totals. Each priority zone was linked to its nearest rain gauge,

matching NDII change values and precipitation values enabling spatiotemporal comparison. In 2020, when annual rainfall was low (8.71 centimeters), NDII values were positive across target areas—indicating that dry antecedent conditions facilitated higher moisture absorption. Conversely, in 2022, with significantly higher rainfall (37.90 centimeters), NDII values turned negative, suggesting saturated soils limited further infiltration. These trends affirm NDII's reliability as a gauge-independent soil moisture proxy during moments of moisture stress—particularly valuable for watershed restoration planning in semi-arid environments with sparse instrumentation.

While NDII proved to be a powerful proxy for soil moisture, further improvements to spatial resolution and morphological detail could amplify its utility for long-term restoration.

Future Enhancements

Future iterations of this model would benefit from incorporating higher-resolution imagery to enhance channel characterization. Fine-scale detection of stream incision, channel width variability, and riffle-pool sequences could improve both the placement and longevity of erosion control structures. These features inform energy dissipation patterns, bank stability, and sediment transport, allowing for design choices that align more closely with geomorphic processes.

These proposed refinements underscore a broader shift toward precision-based restoration, where geospatial modeling guides—but does not replace—on-the-ground expertise.

Implications & Field Validation

This study reframes conventional restoration planning from anecdotal site selection to spatially explicit, increasing ecological confidence in ORD deployment. By

integrating NDII with terrain-based analyses, land managers are empowered to make informed decisions rooted in both ecological need and logistical feasibility. The NDII-driven framework elevates restoration strategies, identifying chronically dry zones where ORDs can enhance infiltration and resilience.

While data-driven modeling significantly narrows down target areas, on-site field validation remains indispensable. Field evaluations allow practitioners to assess real-world conditions—such as channel morphology, soil health and vegetation dynamics—to ensure proposed interventions enhance the ecosystem without causing unintended degradation. Spatial modeling enables efficient site selection by refining the pool of potential restoration areas—establishing a scientifically prioritized shortlist that is subsequently validated through detailed ground truthing.

LIST OF REFERENCES

- Cuenca Los Ojos, Borderlands Restoration Network, & Biophilia Foundation. (2021). Rock detention structures: Restoring watersheds for wildlife. <https://www.biophiliafoundation.org/wp-content/uploads/Rock-Detention-Structures-Introduction-1.pdf>
- Esri. (n.d.). Predict floods with unit hydrographs. Learn ArcGIS. <https://learn.arcgis.com/en/projects/predict-floods-with-unit-hydrographs/>
- Gooden, J., & Pritzlaff, R. (2021). Dryland watershed restoration with rock detention structures: A nature-based solution to mitigate drought, erosion, flooding, and atmospheric carbon. *Frontiers in Environmental Science*, 9, Article 679189. <https://doi.org/10.3389/fenvs.2021.679189>
- Hardisky, M. A., Klemas, V., & Smart, R. M. (1983). The influence of soil salinity, growth form, and leaf moisture on the spectral radiance of *Spartina alterniflora* canopies. *Photogrammetric Engineering and Remote Sensing*, 49(1), 77–83. https://www.asprs.org/wp-content/uploads/pers/1983journal/jan/1983_jan_77-83.pdf
- Heilman, P., Archer, S. R., Williams, C. J., Scott, R. L., Goodrich, D. C., Holifield Collins, C., Naito, A. T., & Ponce-Campos, G. E. (2024). The LTAR grazing land common experiment at Walnut Gulch Experimental Watershed. *Journal of Environmental Quality*, 53(5), 1037–1047. <https://doi.org/10.1002/jeq2.20643>
- Jacobson, P. J., Jacobson, K. M., Angermeier, P. L., & Cherry, D. S. (2000). Hydrologic influences on soil properties along ephemeral rivers in the Namib Desert. *Journal of Arid Environments*, 45(1), 21–34. <https://doi.org/10.1006/jare.1999.0619>
- Korres, W., Reichenau, T. G., Fiener, P., Koyama, C. N., Bogen, H. R., Cornelissen, T., Baatz, R., Herbst, M., Diekkrüger, B., Vereecken, H., & Schneider, K. (2015). Spatio-temporal soil moisture patterns – A meta-analysis using plot to catchment scale data. *Journal of Hydrology*, 520, 326–336. <https://doi.org/10.1016/j.jhydrol.2014.11.042>
- Leopold, A. (1933). The Virgin Southwest. In S. L. Flader & J. B. Callicott (Eds.), *The River of the Mother of God and Other Essays by Aldo Leopold*. University of Wisconsin Press.
- Levick, L. R., Fonseca, J., Goodrich, D. C., Hernandez, M., Semmens, D. J., Leidy, R. A., Scianni, M., Guertin, D. P., Stromberg, J., Tluczek, M., & Kepner, W. G. (2008). The ecological and hydrological significance of ephemeral and intermittent streams in the arid and semi-arid American Southwest (EPA/600/R-08/134). U.S. Environmental Protection Agency & USDA/ARS Southwest Watershed Research Center. https://www.epa.gov/sites/default/files/2015-03/documents/ephemeral_streams_report_final_508-kepner.pdf

- Maestas, J. D., Conner, S., Zeedyk, B., Neely, B., Rondeau, R., Seward, N., Chapman, T., With, L., & Murph, R. (2018). Hand-built structures for restoring degraded meadows in sagebrush rangelands: Examples and lessons learned from the Upper Gunnison River Basin, Colorado (Range Technical Note No. 40). USDA Natural Resources Conservation Service. https://www.wfw.org/wp-content/uploads/2018/05/CO-NRCS_Range_Technical_Note_40_Gunnison_Zeedyk-Structures_5-18.pdf
- Maidment, D. R., Olivera, F., Calver, A., & Wallis, S. (1996). Unit hydrograph derived from a spatially distributed velocity field. *Hydrological Processes*, 10(6), 831–844. [https://doi.org/10.1002/\(SICI\)1099-1085\(199606\)10:6<831::AID-HYP374>3.0.CO;2-N](https://doi.org/10.1002/(SICI)1099-1085(199606)10:6<831::AID-HYP374>3.0.CO;2-N)
- Norman, L. M. (2020). Ecosystem services of riparian restoration: A review of rock detention structures in the Madrean Archipelago Ecoregion. *Air, Soil and Water Research*, 13, 1178622120946337. <https://doi.org/10.1177/1178622120946337>
- Norman, L. M., Ruddell, B. L., Tosline, D. J., Fell, M. K., Greimann, B. P., & Cederberg, J. R. (2021). Developing climate resilience in aridlands using rock detention structures as green infrastructure. *Sustainability*, 13(20), 11268. <https://doi.org/10.3390/su132011268>
- Osterkamp, W. R., & Nichols, M. H. (2006). Geomorphic and physiographic characteristics and processes of the Walnut Gulch Experimental Watershed, Arizona, United States. In *Proceedings of the Conference on Management of Landscapes Disturbed by Channel Incision* (pp. xxx–xxx). U.S. Geological Survey.
- Southwest Watershed Research Center. (2003). *Walnut Gulch Experimental Watershed* [Brochure]. United States Department of Agriculture. <https://www.ars.usda.gov/ARSUserFiles/20221000/WGBrochure.pdf>
- Sriwongsitanon, N., Gao, H., Savenije, H. H. G., Maekan, E., Saengsawang, S., & Thianpopirug, S. (2016). Comparing the Normalized Difference Infrared Index (NDII) with root zone storage in a lumped conceptual model. *Hydrology and Earth System Sciences*, 20(8), 3361–3377. <https://doi.org/10.5194/hess-20-3361-2016> University Corporation for Atmospheric Research. (n.d.). *CEOP Walnut Gulch hydrology reference site*. <https://archive.eol.ucar.edu/projects/ceop/dm/hydro/sites/walnut/>
- U.S. Geological Survey. (2024, April 19). *Lessons learned using stream morphology and simple erosion control structures* [Video transcript]. U.S. Geological Survey. <https://www.usgs.gov/media/videos/lessons-learned-using-stream-morphology-and-simple-erosion-control-structures-past>
- Watts, C. J., Scott, R. L., Garatuza-Payan, J., Rodriguez, J. C., Prueger, J. H., Kustas, W. P., & Douglas, M. (2007). Changes in vegetation condition and surface fluxes

during NAME 2004. *Journal of Climate*, 20(9), 1810–1820.
<https://doi.org/10.1175/JCLI4097.1>

Wilson, N. R., & Norman, L. M. (2018). Analysis of vegetation recovery surrounding a restored wetland using the normalized difference infrared index (NDII) and normalized difference vegetation index (NDVI). *International Journal of Remote Sensing*, 39(10), 3243–3274. <https://doi.org/10.1080/01431161.2018.1437297>

APPENDIX A

METADATA TABLES

Table A1. Shuttle Radar Topography Mission (SRTM) 1 Arc-Second Global DEM

Field	Description
Official Name	SRTM 1 Arc-Second Global DEM
Year of Publication/Update	Initially published in 2003; updated periodically
Author/Owner	United States Geological Survey (USGS)
Repository URL	https://earthexplorer.usgs.gov
Description	30 m resolution DEM derived from radar interferometry; supports slope and watershed modeling
Coordinate System	WGS84 (Geodesic model), Horizontal Datum: WGS84, Vertical Datum: EGM96, EPSG: 4326
Projection System	Unprojected (geographic coordinates)
Spatial Resolution	30 meters
Type of Geometry	Raster

Table A2. Landsat 8–9 OLI/TIRS Collection 2 Level-2 Surface Reflectance Imagery

Field	Description
Official Name	Landsat 8–9 OLI/TIRS Collection 2 Level-2 Surface Reflectance
Year of Publication/Update	2020–2022 (scenes used), Collection updated regularly
Author/Owner	USGS/NASA
Repository URL	https://earthexplorer.usgs.gov
Description	Atmospherically corrected surface reflectance bands; used for NDII and temporal analysis
Coordinate System	WGS84 (Geodesic model), Horizontal Datum: WGS84, Vertical Datum: N/A, EPSG: 4326
Projection System	WGS 1984 UTM Zone 12N (EPSG: 32612)
Spatial Resolution	30 meters
Type of Geometry	Raster

Table A3. SWRC Flume and Rain Gauge Locations

Field	Description
Official Name	SWRC Flume and Rain Gauge Point Locations
Year of Publication/Update	Varies per instrument; maintained actively
Author/Owner	USDA ARS Southwest Watershed Research Center
Repository URL	https://swrc-usdaars.hub.arcgis.com
Description	Georeferenced points for instrumentation across WGEW; includes metadata like elevation and type

Coordinate System	NAD83 (Geodesic model), Horizontal Datum: NAD83, Vertical Datum: N/A, EPSG: 4269
Projection System	UTM Zone 12N or state plane
Spatial Resolution	N/A
Type of Geometry	Vector (Point)

Table A4. Arizona Rivers Layer

Field	Description
Official Name	AZ Rivers (Hydrographic Features)
Year of Publication/Update	Not explicitly listed; likely maintained and updated by UArizona GIS (2024-2025)
Author/Owner	University of Arizona GIS (UAGIS)
Repository URL	https://uagis.maps.arcgis.com/apps/mapviewer/index.html?webmap=a3873be87f794ad985d52fca48e1eeb1
Description	Statewide hydrographic features; used for spatial orientation within study area
Coordinate System	WGS 1984 (Geodesic Model), Horizontal Datum: D_WGS_1984, Vertical Datum: N/A, EPSG: 4269
Projection System	WGS 1984 Mercator (Auxiliary Sphere); (EPSG: 3857)
Spatial Resolution	N/A
Type of Geometry	Vector (Polyline)

Table A5. Primary and Secondary Roads (TIGER/Line 2024)

Field	Description
Official Name	TIGER/Line Roads Dataset – Cochise County, AZ
Year of Publication/Update	2024
Author/Owner	U.S. Census Bureau
Repository URL	https://www.census.gov/cgi-bin/geo/shapefiles/index.php?year=2024&layergroup=Roads
Description	Vector lines representing primary/secondary roads used to score accessibility in modeling
Coordinate System	NAD83 (Geodesic model), Horizontal Datum: NAD83, EPSG: 4269
Projection System	N/A
Spatial Resolution	N/A
Type of Geometry	Vector (Line)

Table A6. Rain Gauge Data – Tucson ARS Digital Aggregate Portal

Field	Description
Official Name	Tucson ARS Rain Gauge Digital Records
Year of Publication/Update	Updated continuously
Author/Owner	USDA Agricultural Research Service
Repository URL	https://www.tucson.ars.ag.gov/dap/digital/aggregate.asp##
Description	Long-term rainfall records with aggregated statistics; supports validation of NDII and trends
Coordinate System	N/A
Projection System	N/A
Spatial Resolution	N/A
Type of Geometry	Tabular/Point data